Yong CHEN[1], Jun TANG[1], Dong-sheng CAI[1], Xia LIU[2]

School of Energy Science and Engineering, University of Electronic Science and Technology of China(1)
School of Electrical and Information Engineering , Xihua University(2)

Torque Ripple Reduction of Brushless DC Motor on Current Prediction and Overlapping Commutation

Abstract. *Based on the analysis of the principle of torque ripple with commutation time for brushless DC motor, this paper proposes a method to restrain commutation torque ripple. This method is an improved predictive current control. First, an expression is built about the torque ripple during commutation time. After analysis, the non-commutation phase current is related to torque ripple. Then, a kind of control strategy is designed. A controller is designed with improved predictive current approach to restrain the torque ripple. Next, the model and controllers are implemented in Simulink environment and numerical simulations are performed. Finally, in order to compare the performance of the proposed controller, experiments on other regular controllers are represented on PWM-ON modulation. The designed controller demonstrates much better performance than that of regular PWM-ON modulation controller under tests. Meanwhile, the effect of simulation indicates that the controller is adaptive for speed variation.*

Streszczenie. *W artykule zaproponowano metodę zmniejszenia zafalowań momentu powodowanego komutacją w bezszczotkowym silniku DC. Zakłada się, że niekomutacyjny prąd fazowy jest miara tych zafalowań. Zaprojektowany sterownik bazuje na przewidywaniu prądu. (**Zmniejszenie zafalowań momentu w bezszczotkowym silniku DC metodą przewidywania prądu i nakładającej się komutacji**)*

Keywords: Brushless DC motor,Torque ripple, Current prediction method, Overlapping commutation.
Słowa kluczowe: silnik bezszczotkowy, zafalowania momentu, komutacja

Introduction

Brushless DC motor has been widely used due to its features-simple control, low noise, high power density, high output torque, etc. However, torque ripple is generated in commutation intervals because of the presence of armature inductance of brushless DC motor which deteriorates the precision of position control and speed control of brushless DC motor. Therefore, restraining commutation torque ripple turns into the hotpot and difficult point of research on brushless DC motor [1-2].

To reduce commutation torque ripple, the literature [3] used a proper duty-ratio control strategy based on deadbeat current control to calculate a pulse width modulation duty ratio for different speed. However, it is typically relied on the current sensor and its dynamic response. The literature adopted the hysteretic current to control the non-commutation phase current directly to reduce commutation torque ripple[4]. Nevertheless, it can only resolve the issue of high speed torque ripple and the effect is not ideal for low speed operation. The Kalman filter was used to minimize torque ripple in literature [5]. It is not required to know the harmonic distribution of back-EMF precisely in advance and can compensate errors of measurement and model. Thus, it can result in high-precision control. Unfortunately, the control algorithm is more complicated and harder for realization compared with common methods. Therefore, commutation torque ripple is the key point of study in this field recently.

The focus of this paper is considered to solve the problem of commutation torque ripple in high speed range and design a method easily to implement in engineering to reduce torque ripple. Current prediction method is typical of high control accuracy, controllable and easy to implement [6-7]. However, due to the different characteristics of torque ripple in high and low speed operation [8], it is required to design different rules of current prediction. The predictive current rules are particularly sensitive to the operating condition and dynamic parameters, which summarily means it is un-adaptive. It is a trend to explore adaptive controllers to restrain torque ripple for the whole speed ranges in practice. Hence, this paper designs a unique controller suitable for the diversification of torque ripple using an improved current prediction method.

The rest of the paper is organized as follows. The reasons of commutation for commutation torque ripple will be presented Section II, followed by the design of improved current prediction rules and controllers in Section III. In Section IV the designed controllers is implemented in Simulink environment and numerically simulated. Also the performance of the designed controllers in this paper is tested and compared with that of regular PWM-ON modulation controllers. Section □ concludes the paper.

Analysis of commutation torque ripple

When the brushless DC motor works in three-phase six-state 120° PWM mode, the currents don't commutate instantaneously due to the existence of inductance of stator phase windings. As a result, the slope of current of incoming and outgoing phase is different during commutation intervals, which causes the change of non-commutating phase current. According to equation (1), the variation of winding current leads to changes of torque without considering the speed and back EMF. That is torque ripple generated during the commutation intervals.

$$Te = \frac{e_a i_a + e_b i_b + e_c i_c}{\omega} \tag{1}$$

where e_a , e_b , e_c are back EMF of phase A, B, C, and i_a , i_b , i_c are phase current. Also, Te is the electromagnetic torque and ω is the speed of the rotor.

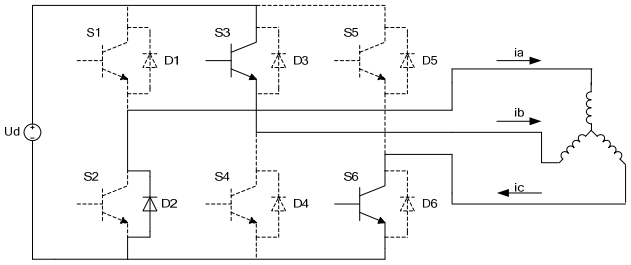

Fig.1.Equivalent circuit and flowing currents in certain commutation interval

The equivalent model of motor and controllers is shown in Fig.1. Commutation torque can be illustrated by the

following analysis where the commutation of the current from phase A to phase B is considered. This current transfer is done by switching off S1 and switching on S3 with S6 remaining on. The status of commutation is shown in Fig. 1 where phase A is the outgoing phase, phase B is the incoming phase and phase C is the non-commutating phase. Also, the flow of current is described. For the electrical model, we consider the equation of the motor as

$$(2)\quad \begin{bmatrix} U_a \\ U_b \\ U_c \end{bmatrix} = \begin{bmatrix} 0 \\ U_d \\ 0 \end{bmatrix} = \begin{bmatrix} R_a & 0 & 0 \\ 0 & R_b & 0 \\ 0 & 0 & R_c \end{bmatrix} \begin{bmatrix} i_a \\ i_b \\ i_c \end{bmatrix} + \left(L \cdot \frac{d}{dt} \begin{bmatrix} i_a \\ i_b \\ i_c \end{bmatrix} \right) + \begin{bmatrix} e_a \\ e_b \\ e_c \end{bmatrix} + \begin{bmatrix} U_N \\ U_N \\ U_N \end{bmatrix}$$

where U_a, U_b, U_c represent the voltage of phase A, B, C, respectively, and U_d is dc-link voltage. The variables R_a, R_b, R_c are resistances of phase A, B, C (the windings of phase A, B,C are considered to be symmetrical, thus $R_a = R_b = R_c = R$). The variables i_a, i_b and i_c are phase currents, L is self-inductance excepting mutual inductance, and U_N is neutral voltage. Also, e_a, e_b and e_c are the back EMF of phase A, B, C back EMF, during the commutation, e_a, e_b, e_c can be shown as $e_a = e_b = E_{\mathrm{m}}$, $e_c = -E_m$, where E_m represents the peak value of back EMF.

$$(3)\quad i_a + i_b + i_c = 0$$

According to (2) and (3), the line-to-line voltage can be calculated as

$$(4)\ U_{ac} = U_a - U_c = R \times (i_a - i_c) + L(\frac{di_a}{dt} - \frac{di_c}{dt}) + 2E_m = 0$$

Similarly,

$$(5)\ U_{bc} = U_b - U_c = R \times (i_b - i_c) + L(\frac{di_b}{dt} - \frac{di_c}{dt}) + 2E_m = U_d$$

In equation (5), i_a, i_b, i_c are all variables. To simplify the equation, $i_b = -(i_a + i_c)$ is substituted into equation (5),

$$(6)\quad R \times (i_a + 2i_c) + L(\frac{di_a}{dt} + 2\frac{di_c}{dt}) - 2E_m + U_d = 0$$

It is obtained from the equation (4) and (6),

$$(7)\quad U_{ac} = -3R \times i_c - 3L\frac{di_c}{dt} + 4E_m - U_d = 0$$

The effect of R can be neglected as the PWM period is much shorter than the electrical time constant L/R [1]. Then the equation (7) can be simplified as

$$(8)\quad i_c = i_{c0} + \frac{4E_m - U_d}{3L}$$

where, i_{c0} is the initial current value of commutation interval.

Similarly,

$$i_b = i_{b0} + \frac{2(U_d - E_m)}{3L} \qquad i_a = i_{a0} - \frac{(U_d + 2E_m)}{3L},$$

From Fig.1, before commutation the motor works in a steady state, as a result, the initial value of current can be shown as $i_{a0} = i_0$, $i_{b0} = 0$, $i_{c0} = -i_0$, where i_0 is a constant.

With the equation of currents and back-EMF, the torque of motor can be shown as

$$Te = \frac{2i_0 E_m}{\omega} + \frac{2E_m}{3L\omega}(U_d - 4E_m)$$

$$Te_0 = \frac{2i_0 E_m}{\omega}$$

Thus the torque ripple during commutation is

$$(9)\quad \Delta T = \frac{2E_m}{3L\omega}(4E_m - U_d)$$

For each BLDC motor, E_m can be written as

$$E_m = \psi_m \omega$$

where ψ_m is the peak of field excitation.

Thus, from the foregoing derivation, the torque ripple is influenced by ω rewritten as:

$$(10)\quad \Delta T = \frac{2\psi_m}{3L}(4\psi_m \omega - U_d)$$

According to (10), the following conclusion can be drawn.

1) On the condition of low speed, the torque keeps decreasing during commutation intervals.

2) On the condition of high speed, the torque tipple is on the trend of rising.

In both cases, the commutation torque pulsation will be produced.

3) If the speed of the rotor is exactly equivalent to $U_d / 4\psi_m$, the pulsation of torque does not exist.

Summarily, the interaction between speed and dc-link voltage is a critical element with torque ripple, however, the problem can't be solved directly though deducing the interaction.

In contrast, the equation of (9) is similar with (8). Apparently, there is some kind of liner relationship between the variation of phase current C and torque ripple, which theoretically provides a practicable solutions by control the variation of phase current C. So, this paper will design controllers to keep i_c constant.

Design of Improved Current Prediction Rules

The control strategy

To keep i_c constant, current prediction is a proper way to modulate control strategy by predicting three phases current variation. As mentioned previously, the predictive current rules are particularly sensitive to the operating condition and dynamic parameters. The rules of current prediction which control the ratio of outgoing phase and keep the incoming phase on change with the speed range. Thus, this paper proposes an improved predictive current controller which separately controls three phases with different ratio regardless of the operating states of motor especially the speed range. Meanwhile, with PWM-ON modulation, the ripple of torque is less compared with other modulation [10]. Generally, the basic control strategy of this paper is PWM-ON control.

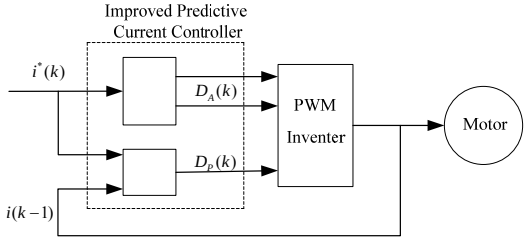

Fig.2. Improved predictive current controller block diagram

A block diagram of the improved predictive control strategy applied to the current control for a three-phase inverter is shown in Fig. 2.

The current control is performed in the following steps.

1) The value of the reference current $i^*(k)$ is obtained from an outer control loop, and the load current $i(k-1)$ is measured.

2)Through $i^*(k)$, $i(k-1)$ and other measured parameters, the duty ratio of control waves is calculated.

3)During the commutation, the incoming and outgoing phase are controlled by $D_A(k)$ .Besides,the PWM determined by the predictive current of non-commutation phase and the non-commutation phase is controlled by the predictive current and real current in previous period of non-commutation phase.

Proceeding of calculation

As shown in Fig.1, phase A is the outgoing phase, phase B is the incoming phase and phase C is the non-commutating phase. In this commutation intervals, considering the control approach proposed in this paper, the switch S3 turned on is controlled by duty ratio $D_A(t)$ while the switch S1 turned off is modulated by duty ratio $D_A(t)$. Meanwhile, the switch state and equivalent circuit are shown in Fig.3. Then, the voltage equation of three windings with phase variables can be expressed as:

$$(11)\quad \begin{bmatrix} U_a \\ U_b \\ U_c \end{bmatrix} = \begin{bmatrix} U_d \times D_A(t) \\ U_d \times D_A(t) \\ 0 \end{bmatrix} = R \times \begin{bmatrix} i_a \\ i_b \\ i_c \end{bmatrix} + L \times \frac{d}{dt} \times \begin{bmatrix} i_a \\ i_b \\ i_c \end{bmatrix} + \begin{bmatrix} e_a \\ e_b \\ e_c \end{bmatrix} + \begin{bmatrix} U_N \\ U_N \\ U_N \end{bmatrix}$$

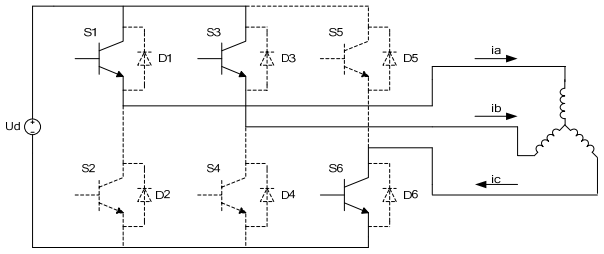

Fig.3. Equivalent circuit and flowing currents based on current prediction method

According to $i_a + i_b + i_c = 0$, neutral voltage U_N calculated by the equation (11) is shown as equation (12).

$$(12)\quad U_N = (2U_d \times D_A(t) - E_m) \Big/ 3$$

After substituting equation (12) into (11), it is obviously that i_a , i_b , i_c have direct relationship with duty ratio $D_A(t)$, as shown in equations (14) and (13).

$$(13)\quad L\frac{di_a}{dt} = U_d \times D_A(t) - R \times i_a - e_a - \frac{2U_d \times D_A(t) - E_m}{3}$$

$$(14)\quad L\frac{di_b}{dt} = U_d \times D_A(t) - R \times i_b - e_b - \frac{2U_d \times D_A(t) - E_m}{3}$$

As demonstrated in section Ⅱ, to restrict torque ripple, non-commutation phase current i_c should be kept constant. So the slopes of phase currents are drawn by

$$(15)\quad \frac{di_a}{dt} + \frac{di_b}{dt} = -\frac{di_c}{dt} = 0$$

From (12), (13) and (14), the duty ratio $D_A(t)$ can be arranged as

$$(16)\quad D_A(t) = (4E_m - 3R \times i_c) \Big/ 2 \times U_d$$

After discretization, $D_A(t)$ can be rewritten as:

$$(17)\quad D_A(k) = (4E_m - 3R \times i^*(k)) \Big/ 2 \times U_d$$

where, $i^*(k)$ is the predictive current of non-commutation phase.

According to equation (17), the predictive current $i^*(k)$ determined by the $D_A(k)$ is the optimal current of phase C. In this commutation interval, the terminal voltage of non-commutation phase C is $V^*(k)$, which is shown as

$$(18)\quad V^*(k) = R \times i^*(k) + L \times \frac{i^*(k) - i(k-1)}{T} + e(k) + U_N$$

Where, T is sampling period of current.

From (12) and (18), $V^*(k)$ is shown as

$$(19)\quad V^*(k) = R \times i^*(k) + L \times \frac{i^*(k) - i(k-1)}{T} + e(k) + \frac{2U_d \times D_A(k) - E_m}{3}$$

where, $V^*(k)$ is the voltage applied to the non-commutation phase to drive the non-commutation phase current reaching to predictive current $i^*(k)$.

$$(20)\quad D_p(k) = \frac{V^*(k)}{U_d}$$

From (19) and (20), finally $D_p(k)$ is calculated as:

$$(21)\quad D_p(k) = \frac{3R \times i^*(k) + 3L \times \frac{i^*(k) - i(k-1)}{T} - 4E_m}{3U_d} + \frac{2D_A(k)}{3}$$

In Fig.4, the control strategy of improved predictive current method is shown compared with PWM-ON modulation method. The aim of the proposed method is to keep the non-commutation phase current constant and the predictive current which is not imaginary is exactly the current needed to be kept constant. The proposed control strategy is theoretically demonstrated that, during the commutation, the incoming and outgoing phases are controlled by the PWM which is determined by the predictive current of non-commutation phase in equation (17). Meanwhile, the non-commutation phase is controlled by the predictive current and real current in the previous period of non-commutation phase in equation (20).

From the process of reasoning, the proposed method is not related to the speed matter. Thus, this rule achieves optimal performance to restrain torque ripple. Whenever the non-commutation phase currents decrease and increase, the torque can be compensated in the whole speed range.

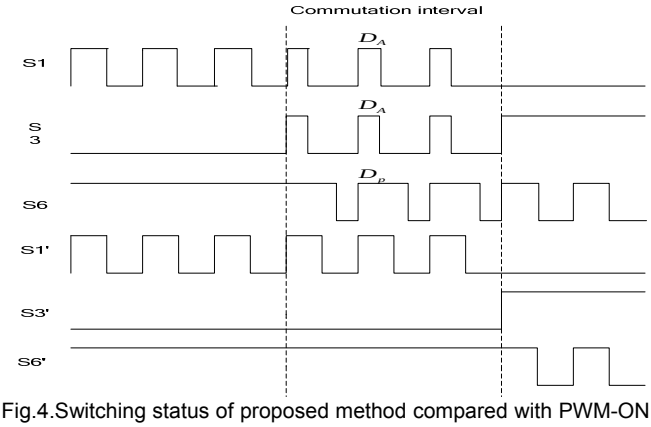

Fig.4.Switching status of proposed method compared with PWM-ON modulation

Simulation and analysis of results

Simulation model

To verify the feasibility of the proposed algorithm, simulations are conducted. A brushless DC motor with a nameplate data shown in Table 1 is considered.

Fig. 5 shows the simulation model of control system which consists of switch logic module, current predictive control module, power module and BLDCM. The parameters used in Fig. 5 are derived from table 1.

Fig. 6 shows the accomplishment of simulation for the improved predictive current method.

In this algorithm, the predictive current is calculated by the equation $Te = \frac{2E}{w} i$, where w is the angular speed, i is non-commutation current. The predictive current is obtained as:

$$i = Te \times w / (2E)$$

Table 1. Parameters of the experimental BLDCM system

Rated Voltage(V)	311
Rated Power(KW)	3.0
Rated Speed(rpm)	3000
Rated Torque(Nm)	12
Pole Number	4
Phase Inductance(mH)	8.5
Phase Resistance(ohm)	2.875
Rotor Inertia(kgm^2)	0.001
PWM Switching Frequence(kHz)	20

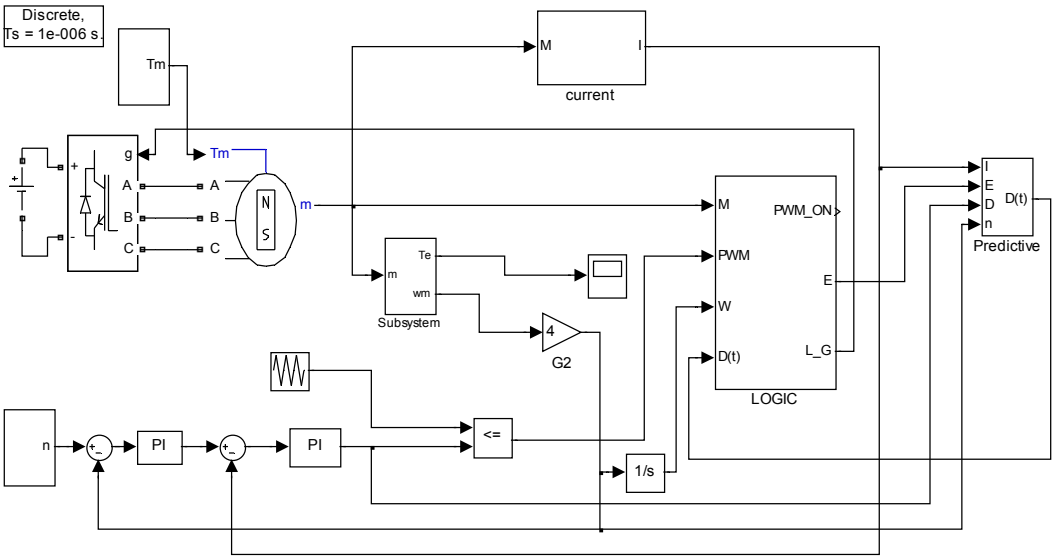

Fig.5.Simulation diagram of control system with improved predictive current method

The predictive current in model is Ik calculated by upper equation. $D(t)$ represents the duty ratio of incoming, outgoing phase and non-commutation phase.

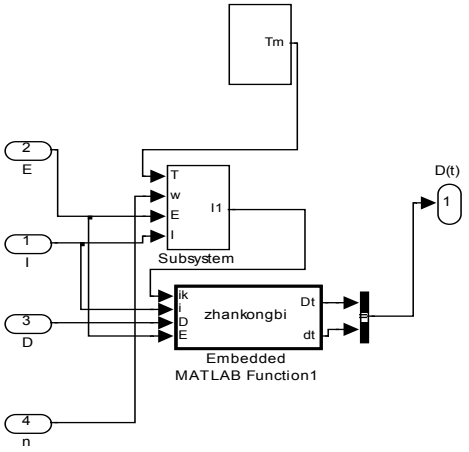

Fig.6.Block diagram of improved predictive current algorithm

The logic module mainly consists of commutation block and logic selection block. The commutation block produces the commutating sequence. The logic selection block distinguishes the working state such as commutation time and normal time. In commutation time, the system is compensated by improved predictive current control while the system is controlled by PWM_ON modulation.

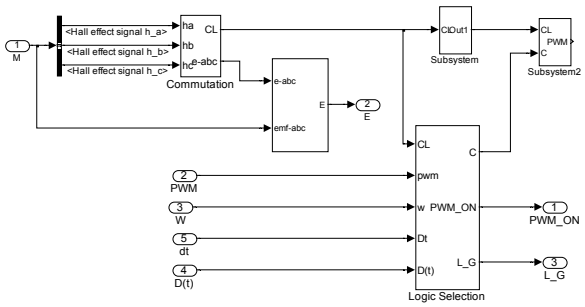

Fig.7. Block diagram of logic module

Analysis of results

To verify the improved predictive current control method, some experiments are presented. The experiments are on the condition of 200r/min, 1000r/m and 3000r/m.

The simulated phase currents of the BLDCM drive system without and with predictive current controller at 200 r/min are compared in Fig. 8 and Fig.9 under the same operating condition. In Fig.8 the phase current dips exist when the motor is controlled by PWM-ON modulation without predictive current controller during commutation intervals. In Fig.9 the phase currents work smoothly with predictive current controller.

As can be seen in Fig.8 and Fig. 9, the current slopes of incoming and outgoing phases during commutation by the proposed method are much closer than those without commutation compensation.

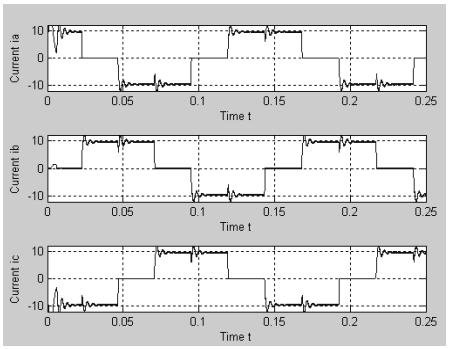

Fig.8.Simulated phase currents at n = 200rpm without predictive current control.

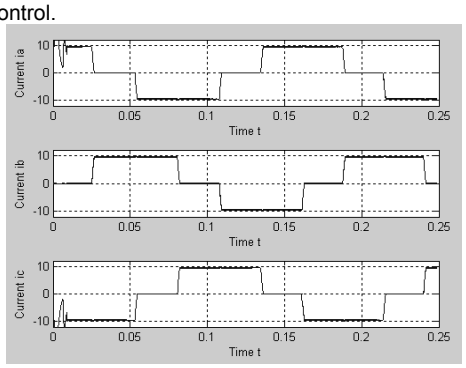

Fig.9.Simulated phase currents at n = 200rpm with predictive current control

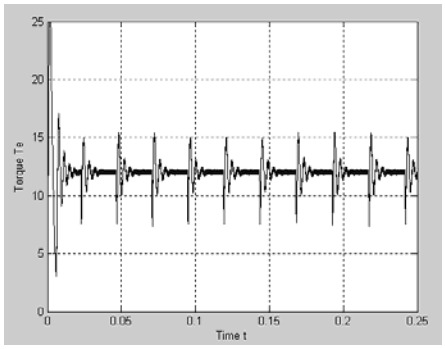

Fig. 10 Simulated electromagnetic torque at n = 200rpm without predictive current control.

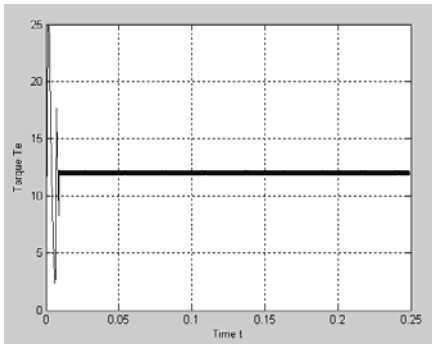

Fig. 11 Simulated electromagnetic torque at n = 200rpm with predictive current control

Fig.10 and Fig.11 show the simulated torque variation without and with the proposed method at 200 r/min. Without consideration of the process of starting, torque ripple existing obviously in Fig.10 is much higher than that in Fig.11. As shown in Fig.11, the torque ripple is prominently suppressed with the proposed method.

The obtained results prove that the proposed predictive control method can be a good alternative to restrict the torque ripple in very low speed range in comparison to the regular methods.

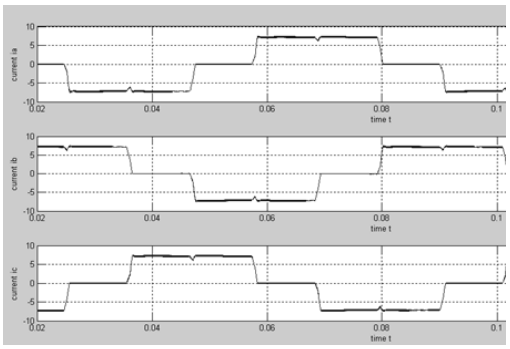

Fig. 12 Simulated phase currents at n = 1000rpm without predictive current control.

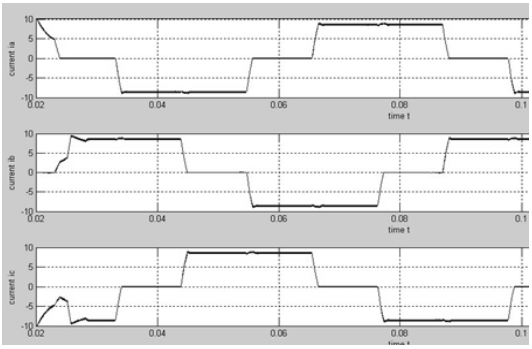

Fig.13 Simulated phase currents at n = 1000rpm with predictive current control

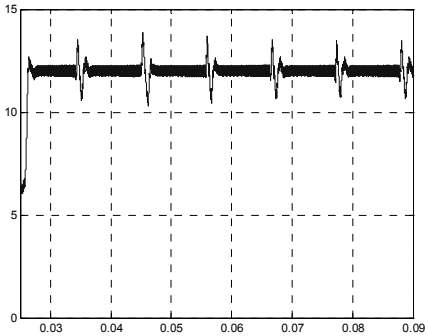

Fig. 14 Simulated electromagnetic torque at n = 1000rpm without predictive current control.

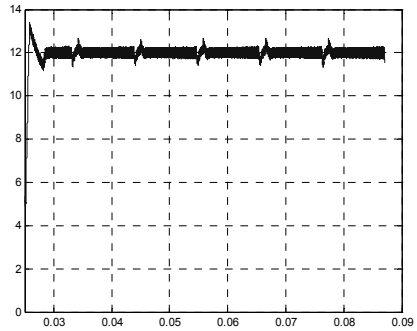

Fig.15 Simulated electromagnetic torque at n = 1000rpm with predictive current control

The simulated phase currents of the BLDCM drive system without and with predictive current controller at 1000 r/min are compared in Fig. 12 and Fig.13 under the same

operating condition. In Fig.12 the phase current dips exist when the motor is controlled by PWM-ON modulation without predictive current controller during commutation intervals. In Fig.13 the phase currents work smoothly with predictive current controller. As can be seen in Fig.12 and Fig. 13, the current slopes of incoming and outgoing phases during commutation by the proposed method are much closer than those without commutation compensation.

Fig.14 and Fig. 15 show the simulated torque variation without and with the use of the proposed method at 1000 r/min. Without consideration of the process of starting, torque ripple existing obviously in Fig. 14 is much higher than that in Fig. 15. As shown in Fig. 15, the torque ripple is significantly suppressed with the proposed method.

The obtained results prove that the proposed predictive control method can be a good alternative to restrict the torque ripple in medium speed range in comparison to conventional ones.

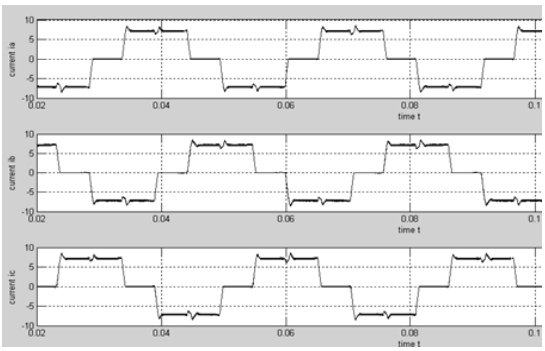

Fig.16 Simulated phase currents at n = 3000rpm with PWM-ON modulation control.

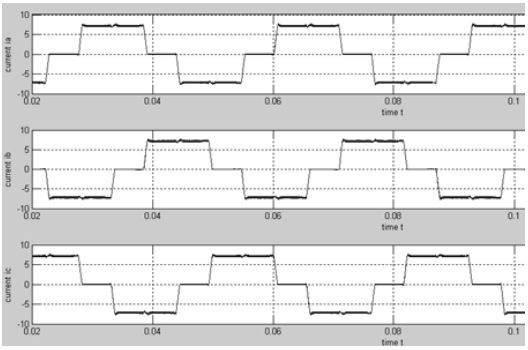

Fig.17 Simulated phase currents at n = 3000rpm with predictive current control

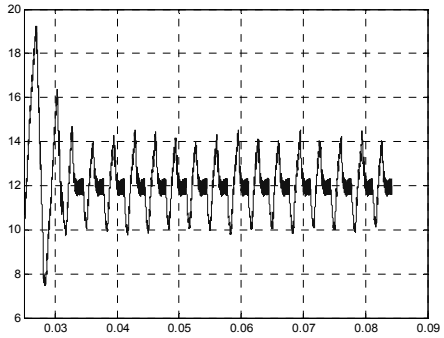

Fig.18 Simulated electromagnetic torque at n = 3000rpm with PWM-ON modulation control.

The simulated phase currents of the BLDCM drive system are shown in Fig.16 and Fig.17 at 3000 r/min with and without the proposed method on the same operating condition. In Fig.16 the performance of phase current is poor when the motor is controlled without the proposed method during commutation intervals. As can be seen in Fig.16 and Fig.17, the current slopes of incoming and outgoing phases during commutation by the proposed method are much closer than those without commutation compensation.

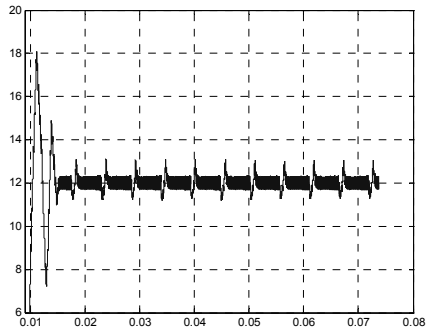

Fig.19 Simulated electromagnetic torque at n = 3000rpm with predictive current control

Fig.18 and Fig.19 show the simulation results of torque without and with the use of the proposed method at 3000 r/min. Torque ripple exists obviously in Fig.18 and the dips and strikes almost exceed 20% of rated torque. In Fig. 19where the proposed compensation algorithm is in use the phase current spike hardly appears.

These figures show that the proposed control technique is very effective at the commutation torque ripple suppression in high speed range.

As shown in Fig. 8, 12 and 16, the phase current ripple in very high speed and very low speed are higher than that in medium speed. Fig. 10, 14 and 18 show the simulated torque variation at 200, 1000 and 3000 r/min. The effect of torque ripple suppression is more obvious at very low speed and very high speed than that at medium speed which indicates that the suppression of torque ripple is harder to deal in very low speed and very high speed. Similarly, the results in paper [10] pointed that the torque ripples would reach to 50% of the average torque at the very low and very high speeds. In contrast, the torque ripples in Fig.11, Fig.15 and Fig.19 are slight.

Therefore, the proposed method is very effective for commutation torque ripple suppression at the high and low speed. This conclusion can even be extended to the entire motor speed range.

Conclusion

In this paper, a commutation torque ripple reduction method has been proposed for brushless dc motor drives using an improved predictive current control method. The proposed method accomplishes successful suppression of the spikes and dips superimposed on the current and torque responses during the commutation intervals. The simulation results indicate that the proposed method is effective in 200r/min, 1000r/m and 3000r/m. and the conclusion can be extended to the whole speed range.

Acknowledgments: This work is partially supported by National Natural Science Foundation of China under grant (61105030), Sichuan Province outstanding youth fund talent training program (09ZQ026-009) and Sichuan Province application foundation project (2009JY0008), China
The Fundamental Research Funds for the Central Universities of China(ZYGX2011J021).

REFERENCES

[1] Shi TN., Guo YT.,Song P., Xia CL., A New Approach of Minimizing Commutation Torque Ripple for Brushless DC Motor Based on DC–DC Converter. *Industrial Electronics, IEEE Transactions on,* 2010,57(10): 3483-3490

[2] Kim DK.,Lee KW.,Kwon BI., Commutation Torque Ripple Reduction in a Position Sensorless Brushless DC Motor Drive. *Power Electronics, IEEE Transactions on*,2006, 21(6): 1762-1768

[3] Song H.J.,Ick C.,Commutation torque ripple reduction in brushless DC motor drivers using a single DC current sensor.*IEEE Trans. On Power Electr*, 2004.19(2): 312-319

[4] Lee DH., Ahn JW. 'A current ripple reduction of a high-speed miniature brushless direct current motor using instantaneous voltage control. *Electric Power Applications, IET*, 2009, 3(2): 85-92

[5] Xiao X., Chen CM., Reduction of Torque Ripple Due to Demagnetization in PMSM Using Current Compensation, *Applied Superconduc-tivity, IEEE Transactions on*,2010,20(3):1068-1071

[6] Gregor R., Barrero F., Toral SL.,.Duran MJ, Arahal MR., Prieto J., Mora JL., Predictive-space vector PWM current control method for asymmetrical dual three-phase induction motor drives,*Electric Power Applications, IET*,2010, 4(1):26-34

[7] Weigold J. ,Braun M.,Predictive Current Control Using Identification of Current Ripple,*Industrial Electronics, IEEE Transactions on*,2008, 55(12):4346-4353

[8] Rodriguez J, Pontt J, Silva C A., Correa P, Lezana P, Cortes P, Ammann U, Predictive Current Control of a Voltage Source Inverter, *Industrial Electronics, IEEE Transactions on*.2007,54(1): 495-498.

[9] Zhang XG, Chen BSi, The different influences of four PWM modes on the commutation torque ripples in sensorless brushless DC motors control system. *Electrical Machines and Systems, ICEMS 2001*(1):575 -578

[10] Carlson R., Lajoie-Mazenc M.,Fagundes J., Analysis of Torque Ripple Due to Phase Commutation in Brushless DC Machines,*IEEE Trans. Ind. Applicant.*1992,28(3):632-638

***Authors**: associate prof. dr Yong CHEN, IEEE member, CSEE member. School of Energy Science and Engineering, University of Electronic Science and Technology of China, E-mail: ychencd@uestc.edu.cn.*

b.eng.Jun TANG, School of Energy Science and Engineering, University of Electronic Science and Technology of China,E-mail: tangajun@gmail.com.

dr Dong-sheng CAI, School of Energy Science and Engineering, University of Electronic Science and Technology of China, E-mail: cai.dsheng@gmail.com.

dr Xia LIU, , School of Electrical and Information Engineering , Xihua University, E-mail: xliu_uestc@yahoo.com;